Available online at www.sciencedirect.com
SCIENCE DIRECT®
PERGAMON
International Journal of Heat and Mass Transfer 46 (2003) 3881–3895
International Journal of HEAT and MASS TRANSFER
www.elsevier.com/locate/ijhmt

The stability of boundary-layer flows under conditions of intense interfacial mass transfer: the effect of interfacial coupling

Iordan A. Halatchev, James P. Denier *

School of Applied Mathematics, The University of Adelaide, Adelaide 5005, Australia

Received 29 September 2001; received in revised form 5 March 2003

Abstract

We consider the linear stability of a boundary-layer flow over a permeable surface under conditions of intense interfacial mass transfer. The stability of the flow is governed by an eigenvalue problem of Orr–Sommerfeld type coupled to a second-order differential equation for the concentration disturbance field through a flux boundary condition at the permeable surface. Previous studies on this problem have ignored the effect on the stability of the flow of this coupling. Curves of neutral stability and the critical Reynolds number for the flow are obtained. These show that the fully coupled system produce critical Reynolds numbers and wave-numbers that, in some cases, differ significantly from those obtained when the disturbance coupling is ignored.

1. Introduction

Our concern is with the stability of boundary-layer flows in the presence of mass transfer across a porous surface. Flows through or over porous media abound, occurring in reactors of all kinds, in many chemical engineering processes, in aeronautics, in waste disposal, in aquifers, in fossil fuel deposits and in high intensity heat and interfacial mass transfer processes. Developments of new technologies in these areas require both improvements in our ability to create adequate mathematical models and in our understanding of the fundamental physical processes involved in the fluid flow.

There are numerous forces which drive mass transfer. By far the most significant of these is the concentration gradient (see Bird et al. [2]). The other important forces are mechanical or external driving forces such as pressure gradients, gravity and electromagnetic forces that may act unequally on various chemical species. The effects of external forces on boundary-layer flows and their hydrodynamic stability have been studied extensively. However, very little research has been conducted into the effect of diffusion on flow instability. In order to focus solely on these effects we will neglect all mechanical driving forces in our analysis.

Our aim is to obtain a more comprehensive understanding of the disturbance dynamics of boundary-layer flows in the presence of diffusion. We focus on the linear stability analysis of a Blasius boundary-layer flow over a semi-infinite, flat, permeable plate across which a concentration gradient exists. One such example is provided by the flow of a fluid containing a chemical species A, at a specified concentration, over a porous surface below which resides the same fluid but with species A at a different concentration. Diffusion through the surface will occur, and its direction will be prescribed by the sign of the concentration difference between the substrate and the upper fluid.

The problem of boundary-layer flow under conditions of interfacial heat and mass transfer, governed by the classical Prandtl equations, the laminar boundary layer convection–diffusion equation and the steady heat transfer equation was first treated by Hartnett and

* Corresponding author.
E-mail addresses: ihalatch@maths.adelaide.edu.au (I.A. Halatchev), jdenier@maths.adelaide.edu.au (J.P. Denier).

0017-9310/03/$ - see front matter © 2003 Elsevier Ltd. All rights reserved.
doi:10.1016/S0017-9310(03)00176-5

Nomenclature

a, b	differential equation coefficients
A	dimensionless wave number
C	concentration
c	dimensionless phase velocity
D	diffusion coefficient
f, g	Blasius similarity function and concentration field, respectively
F, G	disturbance velocity and concentration amplitudes
i	imaginary number
k	parameter
L	characteristic length
M	molecular mass
p	pressure
P	disturbance pressure
Re	Reynolds number
R_δ	Reynolds number based upon boundary-layer thickness
Sc	Schmidt number
t	time
u, v	disturbance velocities in the x- and y-direction
U, V	velocity in x- and y-direction
x, y	Cartesian coordinates along and normal to the plate, respectively
y	normal coordinate
Y	boundary-layer coordinate

Greek symbols

α	wavenumber
β/α	phase velocity
δ	boundary-layer thickness
ϵ	infinitesimally small perturbation parameter
η	similarity variable
θ	mass-transfer parameter
λ	length number
ν	kinematic viscosity
π	pi
ρ	density
φ	dimensionless momentum amplitude
σ	dimensionless concentration amplitude

Subscripts and superscripts

$*$	dimensional quantities
0	conditions of the transferred substance as well as flow conditions
B	boundary-layer flow conditions
crit	critical value of a parameter
max	maximum
min	minimum

Eckert [13]. The system was subject to boundary conditions accounting for foreign fluid injection (with a blowing velocity $V(x,0) \neq 0$). It was shown that in the case when $V(x,0) \sim x^{-1/2}$ the governing equations admit self-similar solutions. These self-similar solutions enabled them to conclude that the velocity, concentration and temperature profiles are greatly influenced by either "suction" or "blowing". For example, the skin-friction demonstrated a significant increase with increasing level of suction.

The stability of such flows was considered by Boyadjiev and co-workers in a series of articles [3–5,12]. These all employed an approximation in which the boundary conditions for the disturbance wave field were linearized. The linearization resulted in a decoupling of the disturbance equations thus leading to a classical eigenvalue problem of Orr–Sommerfeld type. The approximation employed in these works was based upon the observation that the inhomogeneous boundary condition on the vertical disturbance velocity component contains a term proportional to the reciprocal of the Reynolds number. It was argued that even for moderate value of the Reynolds number, this term would be small and hence that the inhomogeneity could be ignored (see expression (15)). Under such an approximation the only way mass transfer can affect the stability of the flow is through its influence on the basic flow; for example, by changing the shape of the velocity profile. Although this approximation serves to capture the qualitative effect of the mass transfer on the stability of the flow, it does not correctly predict the critical parameter values for the onset of instability (values such as the Reynolds number, wave-number and wave-speed). Accurate values of these parameters are necessary if the theory of finite amplitude disturbances in such flows is to be developed. To do this the fully coupled system must be solved. Such is the concern of this work.

Before proceeding to a precise formulation of the problem at hand it is worth noting that problems, that at first glance, appear similar to that considered here are encountered in the study of buoyancy driven flows. In this case the coupling between fluid momentum and an externally applied force, in this case buoyancy due to surface heating, occurs directly in the equations. Representative examples can be found in the work of Gebhart et al. [11] on laminar natural convection flow arising from a steady thermal line source positioned at the leading edge of a vertical adiabatic surface, the work by Lee et al. [9] on natural convection in laminar boundary-layer flows along vertical and horizontal

plates with uniform wall temperature and uniform vectored surface mass transfer, that of Brewster and Gebhart [7] on the stability analysis of a laminar mixed-convection boundary layer adjacent to a vertical isothermal surface and the stability of horizontal mixed convection boundary layer considered by Mureithi et al. [15]. The important difference between the mass transfer problem (the object of the current study) and heat transfer problems is that in the mass transfer problem there is no direct coupling between the field equations themselves; such coupling occurs only through the boundary conditions applied at the surface. This form of coupling requires some care when implementing any numerical scheme to solve the equations governing an infinitesimal disturbance.

The structure of the paper is as follows. In Section 2 we formulate the problem and present some details of the basic boundary-layer flow we will consider. The stability problem is formulated in Section 3 and the fully coupled eigenvalue problem governing the stability of the flow is derived. In Section 4 we describe the salient features of the numerical scheme used to solve the eigenvalue problem of Section 3. Our results are presented in Sections 5 and 6 we present some brief conclusions and possible future directions of investigation.

2. Formulation

Consider the laminar flow of a viscous incompressible fluid over a flat, semi-infinite, permeable plate across which a concentration gradient exists (see Fig. 1). In practice below the surface is a reservoir of fluid which is kept fully mixed so as to ensure that the concentration at the surface remains constant. The concentration difference induces a mass flux at the permeable surface. The rate v_n^* of the induced flow can be defined in terms of the mass flux through the surface as

$$v_n^* = -\frac{MD}{\rho^*}\frac{\partial C^*}{\partial n}, \tag{1}$$

where M is the molecular mass, D is the diffusion coefficient, ρ^* the density of the fluid, C^* the concentration and $\partial/\partial n$ denotes the derivative normal to the permeable surface; in the case of the flat-plate boundary layer $\partial/\partial n = \partial/\partial y^*$ (see expression (19.3–13) of Bird et al. [2]).

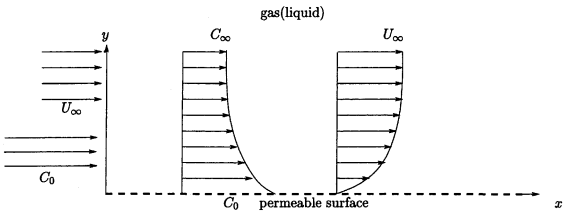

Fig. 1. A schematic description of the flow.

Let x^* and y^* denote Cartesian coordinates aligned along and normal to the plate surface, respectively, U^* and V^* the corresponding velocity components, P^* the pressure, ν the kinematic viscosity, C^* the concentration and ρ^* the fluid density. We will only consider the case of a fluid of constant density. Here an asterisk denotes a dimensional quantity. We define non-dimensional variables according to

$$(x^*, y^*) = L(x, y), \quad t^* = \frac{Lt}{U_\infty}, \quad (U^*, V^*) = U_\infty(U, V),$$
$$C^* = C_\infty^* + (C_0^* - C_\infty^*)C, \quad P^* = \rho^* U_\infty^2 P,$$

where L is a typical length (for example, the distance from the leading edge of the plate), U_∞ the free-stream speed, C_0^* the concentration at $y^* = 0$ and C_∞^* the concentration as $y^* \to \infty$. The resulting non-dimensional equations governing the flow are then

$$\frac{\partial U}{\partial x} + \frac{\partial V}{\partial y} = 0, \tag{2a}$$

$$\frac{\partial U}{\partial t} + U\frac{\partial U}{\partial x} + V\frac{\partial U}{\partial y} = -\frac{\partial P}{\partial x} + \frac{1}{Re}\left(\frac{\partial^2}{\partial x^2} + \frac{\partial^2}{\partial y^2}\right)U, \tag{2b}$$

$$\frac{\partial V}{\partial t} + U\frac{\partial V}{\partial x} + V\frac{\partial V}{\partial y} = -\frac{\partial P}{\partial y} + \frac{1}{Re}\left(\frac{\partial^2}{\partial x^2} + \frac{\partial^2}{\partial y^2}\right)V, \tag{2c}$$

$$\frac{\partial C}{\partial t} + U\frac{\partial C}{\partial x} + V\frac{\partial C}{\partial y} = \frac{1}{ScRe}\left(\frac{\partial^2}{\partial x^2} + \frac{\partial^2}{\partial y^2}\right)C. \tag{2d}$$

In general these must be solved subject to the initial conditions

$$U = 1, \ V = 0, \ C = 1 \quad \text{at } x = 0$$

and boundary conditions

$$U = 0, \ V = -\frac{\theta}{ScRe}\frac{\partial C}{\partial y}, \ C = 1 \quad \text{on } y = 0;$$
$$U \to 1, \ C \to 0 \quad \text{as } y \to \infty. \tag{3}$$

Here $Re = U_\infty L/\nu$ is the Reynolds number, $Sc = \nu/D$ is the Schmidt number and $\theta = M(C_0^* - C_\infty^*)/\rho^*$ is a parameter which characterises the intensity of the mass transfer across the permeable surface (see Ref. [3] for details).

In the limit of large Reynolds number the flow naturally develops a boundary layer of thickness $O(Re^{-1/2})$ attached to the leading edge of the plate. We introduce boundary-layer variables

$$y = Re^{-1/2}Y, \quad U = U_B, \quad V = Re^{-1/2}V_B, \quad C = C_B,$$

where y is the physical coordinate and Y the boundary-layer coordinate. The steady boundary-layer equations are then

$$\frac{\partial U_B}{\partial x} + \frac{\partial V_B}{\partial Y} = 0, \tag{4a}$$

$$U_B \frac{\partial U_B}{\partial x} + V_B \frac{\partial U_B}{\partial Y} = \frac{\partial^2 U_B}{\partial Y^2}, \tag{4b}$$

$$\frac{\partial P_B}{\partial Y} = 0, \tag{4c}$$

$$U_B \frac{\partial C_B}{\partial x} + V_B \frac{\partial C_B}{\partial Y} = \frac{1}{Sc} \frac{\partial^2 C_B}{\partial Y^2}, \tag{4d}$$

where, for simplicity, we have assumed that the free-stream speed is uniform in which case $\partial P_B/\partial x = 0$. The boundary conditions appropriate to this system are, from (3),

$$U_B = 0,\ V_B = -\frac{\theta}{Sc}\frac{\partial C_B}{\partial Y},\ C_B = 1 \quad \text{on } Y = 0;$$
$$U_B \to 1,\ C_B \to 0 \quad \text{as } Y \to \infty. \tag{5}$$

Noting that $C_{BY}(0) < 0$ the mass transfer has the effect of prescribing a blowing or suction velocity at the surface, depending upon whether θ is positive or negative. Our concern is with how this diffusion driven mass-transfer affects the hydrodynamic stability of the flow.

In what follows we will employ a similarity solution to the boundary-layer equations as our basic flow. Introducing the similarity variable $\eta = Y/x^{1/2}$ we find that the boundary-layer equations (4) admit similarity solutions of the form

$$\eta = \frac{Y}{x^{1/2}}, \quad U_B = f'(\eta), \quad V_B = \frac{1}{2\sqrt{x}}(\eta f' - f),$$
$$C_B = g(\eta), \tag{6}$$

where the functions f and g satisfy

$$f''' + \frac{1}{2} f f'' = 0, \quad g'' + \frac{Sc}{2} g' f = 0 \tag{7}$$

subject to the boundary conditions

$$f(0) = \frac{2\theta}{Sc} g'(0),\ f'(0) = 0,\ g(0) = 1;$$
$$f'(\infty) = 1,\ g(\infty) = 0. \tag{8}$$

The two-point boundary-value problem (7)–(8) was solved numerically using a simple shooting technique based upon a fourth-order Runge–Kutta quadrature scheme and Newton–Raphson iteration. Plots of streamwise velocity $f'(\eta)$ and concentration $g(\eta)$ are presented in Fig. 2 for the representative case of $Sc = 0.1$.

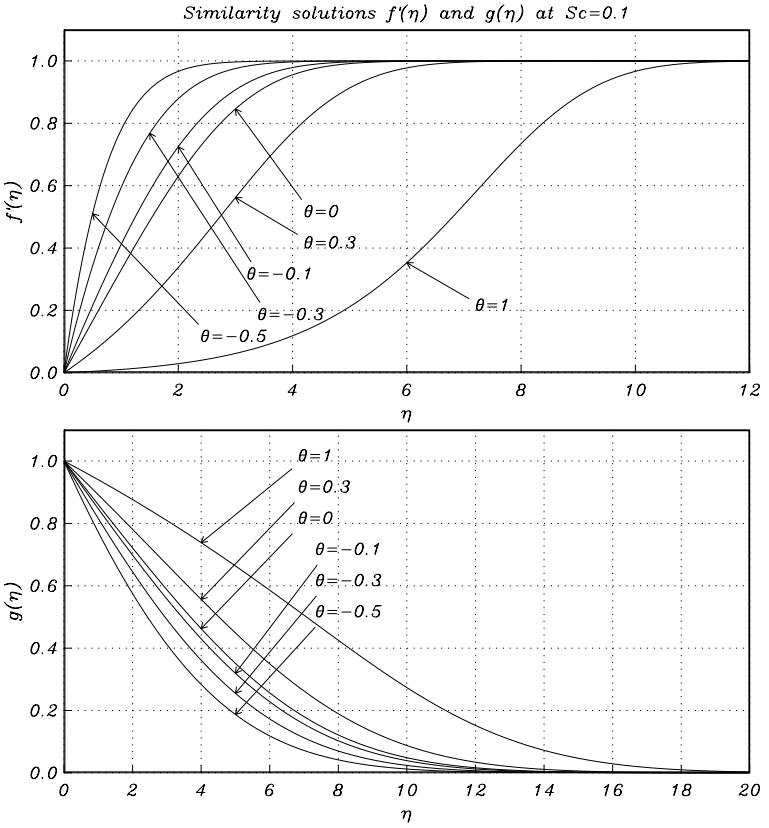

Fig. 2. Graphs of the Blasius function $f'(\eta)$ and the basic concentration $g(\eta)$ versus η at different values of the mass-transfer parameter θ for Schmidt number $Sc = 0.1$.

The effect of mass transfer on the boundary layer has been considered by Boyadjiev and Vulchanov [6] who demonstrated that the secondary flow, with flow rate $f(0)$, does not change the qualitative character of the flow but simply serves to modify the shape of the velocity profile $f'(\eta)$ through the change in the value of the skin friction. The skin friction $f''(0)$ and concentration gradient at the wall $g'(0)$ at different values of the mass-transfer parameter θ and Schmidt number Sc are shown in Fig. 3. These calculations have been carried out for values of the mass-transfer parameter θ within the interval $[-1, 1]$ and for values of the Schmidt $Sc = 0.01$, 0.2, 0.5, 0.7, 1 (corresponding to gas flows) and $Sc = 2$, 25, 50, 100 (corresponding to liquid flows). From Fig. 3 we observe that there is a strong dependency of the skin friction $f''(0)$ on both θ and Sc. At low values of the Schmidt number (note $Sc = \nu/D$), corresponding to a thicker concentration boundary layer, one can expect rapid momentum boundary-layer thickening even at moderately low values of the mass-transfer parameter θ (the case of gas flows). As the concentration boundary-layer thickness decreases, for increasingly higher values of the Schmidt number, the effect of the secondary flux through the surface (the "suction" or "blowing") becomes less significant and the diffusion has little or no impact on the boundary-layer growth as evidenced by the plots of skin friction $f''(0)$ in Fig. 3. It is also apparent that the boundary-layer flow will more readily separate for lower Sc (the gas case). For higher Schmidt number (as occur in liquid flows), the boundary-layer growth is similar to the classical Blasius boundary-layer ($\approx x^{1/2}$) and this behaviour persists even at high values of the mass-transfer parameter θ. The concentration gradient through the interface $g'(0)$ also shows a marked (non-linear) dependency on θ and Sc. Fig. 3 shows that the absolute value of the concentration gradient increases with Schmidt number. This increase is far more pronounced in the "suction" regime than in the "blowing" regime. At fixed values of the mass-transfer parameter θ the concentration gradient decreases with a decrease in Schmidt number Sc. Nevertheless its impact on the boundary-layer growth is significant due to the corresponding increase in the thickness of the concentration boundary layer and its interaction with the hydrodynamic boundary layer.

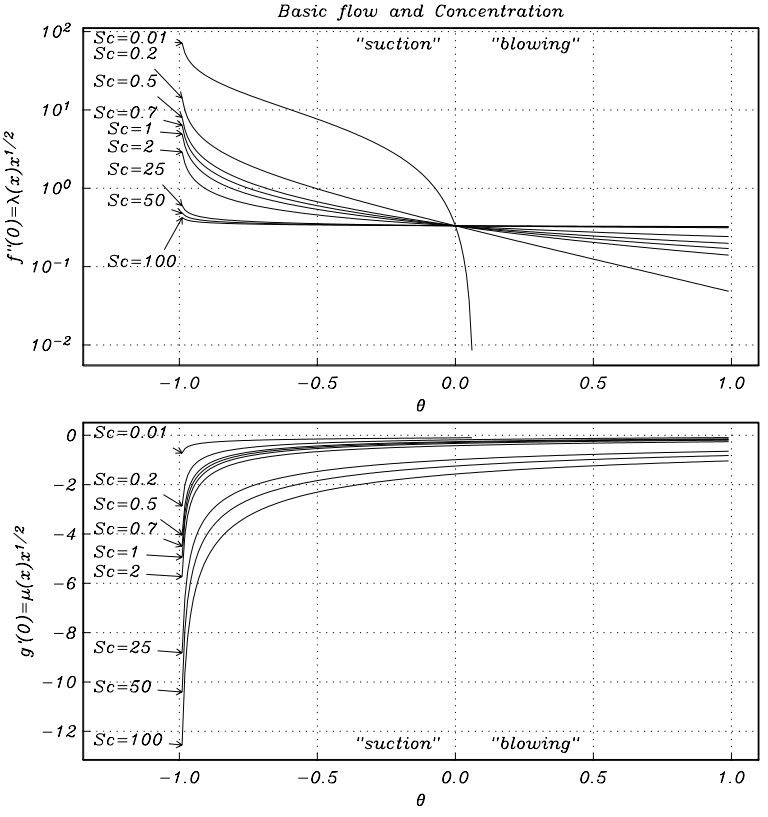

Fig. 3. Graphs of $f''(0)$ and $g'(0)$ versus θ for different values of Sc.

3. Linearized instability of the boundary-layer flow

In order to consider the linear stability of the flow we superimpose an infinitesimally small two-dimensional disturbance on the basic boundary layer. In this case the total flow field is written as

$$(U,V,P,C) = (U_{\mathrm{B}}, Re^{-1/2}V_{\mathrm{B}}, P_{\mathrm{B}}, C_{\mathrm{B}}) + \epsilon(u,v,p,c) + O(\epsilon^2), \tag{9}$$

where ϵ is the infinitesimally small disturbance amplitude. Substituting this expression into the system (2) and linearising with respect to ϵ gives

$$u_x + v_y = 0, \tag{10a}$$

$$u_t + U_{\mathrm{B}}u_x + uU_{\mathrm{B}x} + vU_{\mathrm{B}y} + Re^{-1/2}V_{\mathrm{B}}u_y = -p_x + Re^{-1}(u_{xx} + u_{yy}), \tag{10b}$$

$$v_t + U_{\mathrm{B}}v_x + Re^{-1/2}uV_{\mathrm{B}x} + Re^{-1/2}V_{\mathrm{B}}v_y + Re^{-1/2}vV_{\mathrm{B}y} = -p_y + Re^{-1}(v_{xx} + v_{yy}), \tag{10c}$$

$$c_t + U_{\mathrm{B}}c_x + uC_{\mathrm{B}x} + Re^{-1/2}V_{\mathrm{B}}c_y + vC_{\mathrm{B}y} = Re^{-1}Sc^{-1}(c_{xx} + c_{yy}). \tag{10d}$$

The mean flow in the x-direction is assumed to be influenced by a disturbance which is composed of a number of discrete partial fluctuations, each of which consists of a wave which is propagated in the x-direction (see Schlichting [16]). It is therefore appropriate to represent a single oscillation in the following form

$$(u(x,y), v(x,y), c(x,y)) = (F'(y), -\mathrm{i}\alpha F(y), \mathrm{i}\alpha G(y)) \times \exp[\mathrm{i}\alpha(x - ct)], \tag{11}$$

where $F(y)$ and $G(y)$ are the disturbance amplitudes, α is the (real) stream-wise wavenumber and $c = c_{\mathrm{r}} + \mathrm{i}c_{\mathrm{i}}$ is the complex wave-speed. If $c_{\mathrm{i}} < 0$ the disturbance is damped and the flow deemed to be stable, whereas if $c_{\mathrm{i}} > 0$ the flow is unstable and the disturbance grows exponentially with time.

In order to reduce the disturbance equations to their standard form we make use of the boundary-layer approximation and introduce the factor

$$\delta_* = 1.720\frac{Re}{R_\delta},$$

where $R_\delta = 1.720(xRe)^{1/2}$ is the Reynolds number based on the local boundary-layer thickness (see [3] for full details). Upon substituting expressions (11) into (10), eliminating the pressure terms by cross-differentiation, introducing the similarity variables (6) and taking into account the transformations

$$F^{(n)}(y) = \delta_*^n\varphi^{(n)}(\eta), \quad G^{(n)}(y) = \delta_*^n\sigma^{(n)}(\eta),$$

we obtain the classical Orr–Sommerfeld equation for the momentum disturbance field together with a second-order differential equation for the concentration disturbance field:

$$(f' - c)(\varphi'' - A^2\varphi) - f'''\varphi = -\frac{1.720\mathrm{i}}{AR_\delta}\left\{\varphi^{(iv)} - 2A^2\varphi'' + A^4\varphi - \frac{1}{2}(\eta f' - f)\varphi''' + \frac{1}{2}[(\eta f''' + f'') + A^2(\eta f' - f)]\varphi'\right\}, \tag{12a}$$

$$(f' - c)\sigma + \mathrm{i}g'\varphi = -\frac{1.720\mathrm{i}}{AR_\delta}\left\{\frac{1}{Sc}(\sigma'' - A^2\sigma) - \frac{1}{2}(\eta f' - f)\sigma'\right\}, \tag{12b}$$

where $A = \alpha/\delta^*$. This system must be solved subject to suitable boundary conditions on the disturbance applied at the surface and in the outer limit of the boundary layer. The latter are simply that the disturbance decay into the outer potential flow thus giving in the boundary conditions

$$(\varphi, \varphi', \sigma) \to 0 \quad \text{as } \eta \to \infty. \tag{13}$$

Two of the boundary conditions to be imposed on the surface are no-slip and zero disturbance concentration which yield

$$\varphi'(0) = 0, \quad \sigma(0) = 0. \tag{14}$$

The final boundary condition is obtained from the boundary condition (3) on the total vertical velocity V by substituting $V = Re^{-1/2}V_{\mathrm{B}} + \epsilon v$ and $C = C_{\mathrm{B}} + \epsilon c$, and equating terms of order ϵ. This yields (when transformed to the variables φ, σ and η)

$$\varphi(0) = \frac{1.720\theta}{ScR_\delta}\sigma'(0). \tag{15}$$

System (12) with boundary conditions (13)–(15) constitutes an eigenvalue problem for c_{r} as a function of A and R_δ. The relationship between R_δ and x can be interpreted in the following way; in determining a critical Reynolds number R_δ (beyond which the flow is unstable) we are, in effect, determining a critical position x_{crit} at which the boundary layer becomes linearly unstable to wave-like disturbances.

The system given by (12a) and (12b) is coupled, not through the equations for the velocity and concentration disturbance fields but through the inhomogeneous boundary condition on the vertical disturbance velocity $\varphi(0)$, Eq. (15). As noted earlier, previous work on this problem by Boyadjiev and co-workers [3–5,12] assumed that the parameter θ was small and thus the boundary condition relating $\varphi(0)$ to the disturbance concentration gradient could be approximated by $\varphi = 0$. This assumption has the appealing effect of decoupling the

momentum and concentration fields for the disturbance thus resulting in a classical Orr–Sommerfeld eigenvalue problem for the complex wave-speed. Under this approximation the effect of the interfacial mass transfer on the flow occurs only through the coupling in the basic flow equations. Although capturing the effect of mass transfer on the boundary layer, this approximation cannot correctly account for the forcing of the disturbance momentum transport due to the diffusion through the permeable surface. We emphasise here that the coupling between the momentum and concentration disturbance fields occurs solely through the boundary condition at the permeable surface.

This form of coupling is in contrast to, for example, that which occurs when considering the stability of boundary-layer flows under the influence of buoyancy forces. In this case the coupling occurs between the momentum field and the accompanying temperature field and occurs in the momentum equations (see [7,9,10,15]). This coupling between the field equations arises due to the change in density of the fluid when it is heated; the impact of this change upon the stability of the flow depends upon the degree of thermal energy that is added. This is in contrast to the current problem in which the stability is affected via an energy input due to diffusive mass transfer. There is, in the current model, no direct coupling between the field equations; coupling occurs only through the normal flux boundary condition imposed at the permeable surface. In what follows, in order to capture the correct physics of the flow, we retain this coupling in both the basic boundary layer and the disturbance equations. To determine the stability of the flow we must therefore solve system (12) subject to the full boundary conditions (13)–(15).

As the solution procedure has some important differences over that which could be employed if the boundary conditions were decoupled we will now present the salient details of the numerical method we have used.

4. Numerical method

Our solution strategy is based upon a finite-difference discretisation of the system (12). It is convenient to write the system in the following generic form

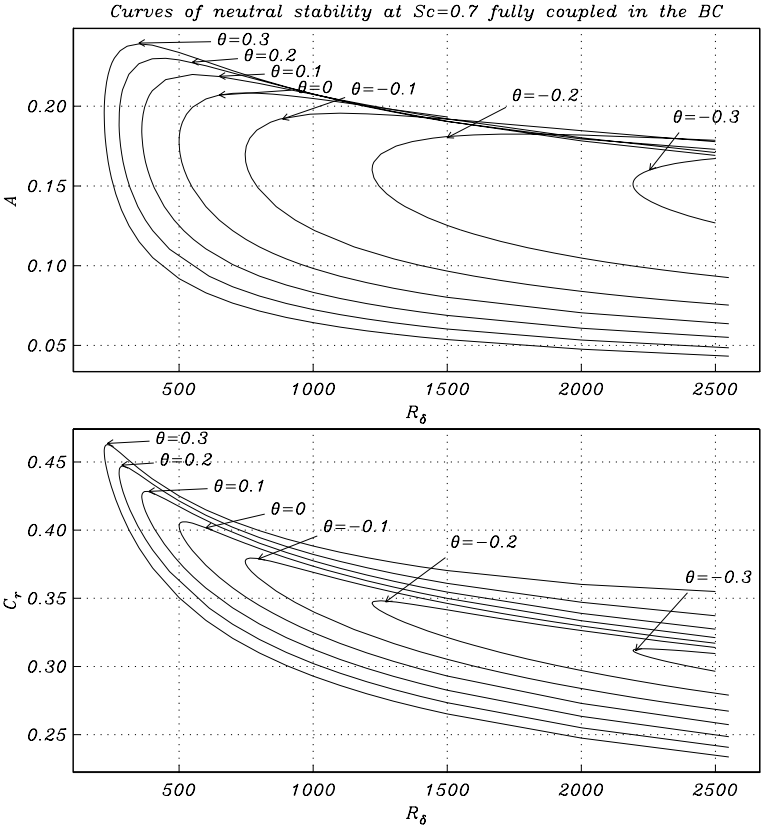

Fig. 4. Curves of neutral stability at $Sc = 0.7$ for different values of θ. The upper plot shows the neutral curves in the (R_δ, A)-plane whereas the lower plot gives the corresponding curves in the (R_δ, c_r)-plane.

$$(D^4 + a_1D^3 + a_2D^2 + a_3D + a_4)\varphi = 0, \tag{16}$$

$$(D^2 + b_1D + b_2)\sigma + b_3\varphi = 0,$$

where D denotes $\mathrm{d}/\mathrm{d}\eta$; the coefficients $a_i = a_i(\eta)$ and $b_j = b_j(\eta)$ $(i = 1,\ldots,4,\ j = 1,\ldots,3)$ are given in Appendix A.

Because of the semi-infinite nature of the domain this must be truncated at some suitably large value of $\eta = \eta_N \gg 1$, chosen to ensure that the variation in the basic flow is negligible at point i.e.

$$f'(\eta_N) = 1, \quad f''(\eta_N) = f'''(\eta_N) = 0,$$
$$\eta_N f'(\eta_N) - f(\eta_N) = k, \quad g(\eta_N) = g'(\eta_N) = 0. \tag{17}$$

Also, as noted by Keller [14], to obtain the correct exponential decay of the eigensolutions as $\eta \to \infty$ we must ensure that the far-field boundary conditions (applied at $\eta = \eta_N \gg 1$) have the correct asymptotic form. These are derived by considering the asymptotic form of the governing equations as $\eta \to \infty$ with the result that the radiation boundary conditions can be written as

$$(D^2 - A^2)\left(D + \frac{1}{4}\sqrt{k^2 + 16\beta_0^2} - \frac{1}{4}k\right)\varphi = 0,$$
$$(D + A)\left(D^2 - \beta_0^2 - \frac{1}{2}kD\right)\varphi = 0, \tag{18}$$
$$\left(D + \frac{1}{4}\sqrt{Sc^2k^2 + 16\beta_1^2} - \frac{1}{4}Sck\right)\sigma = 0,$$

in the limit $\eta \to \infty$. Note that in the far-field the boundary conditions on φ and σ decouple. In the case $k = 0$ (that is ignoring the non-parallel effects arising from the boundary-layer growth) the first two equations in (18) reduce to those obtained by Keller [14] thus providing a useful consistency check on our results.

Our general approach to the solution of the eigenvalue problem governed by (12) and (13)–(15) will be to employ a second-order accurate, finite-difference discretisation of the disturbance equations. Letting φ_j and σ_j denote values of φ and σ at grid point $\eta_j = jh$, discretising the disturbance equations using second-order accurate centered differences [1] yields

$$\mu_1\varphi_{j-2} + \mu_2\varphi_{j-1} + \mu_3\varphi_j + \mu_4\varphi_{j+1} + \mu_5\varphi_{j+2} = 0, \tag{19a}$$

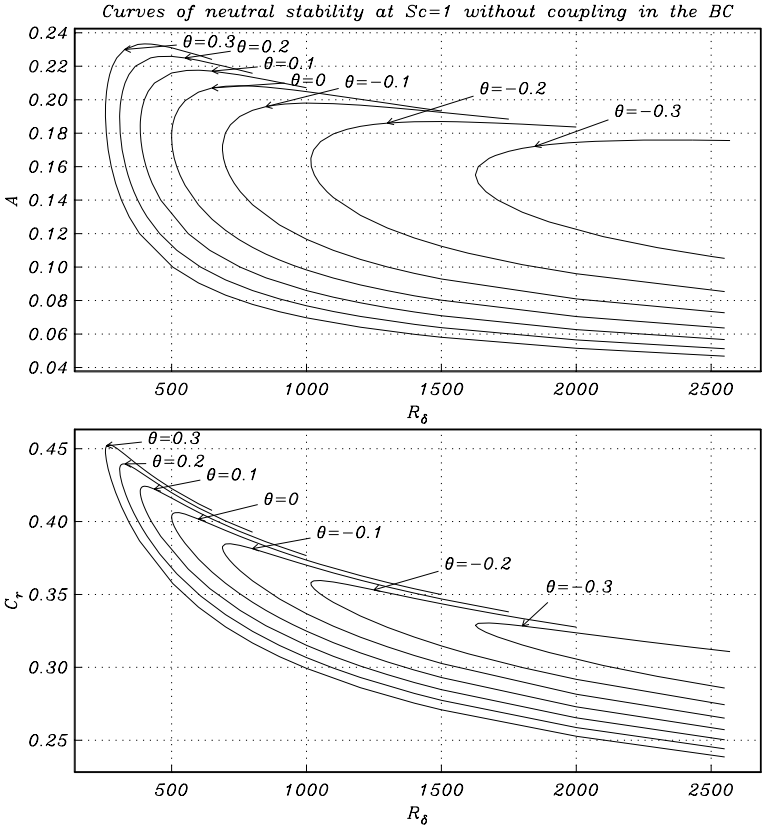

Fig. 5. Curves of neutral stability at $Sc = 1$ for different values of θ. The upper plot shows the neutral curves in the (R_δ, A)-plane whereas the lower plot gives the corresponding curves in the (R_δ, c_r)-plane.

$$\mu_6\sigma_{j-1} + \mu_7\sigma_j + \mu_8\sigma_{j+1} = \mu_9\varphi_j, \tag{19b}$$

for $j = 1, \ldots, N$. Applying the centered difference discretization to the far-field boundary conditions at $\eta = \eta_N$ serves to determine $\varphi_{N+2}, \varphi_{N+1}$ and σ_{N+1} through the relations

$$-\frac{1}{2}\varphi_{N-2} + \zeta_1\varphi_{N-1} - \zeta_2\varphi_N - \zeta_3\varphi_{N+1} + \frac{1}{2}\varphi_{N+2} = 0, \tag{20a}$$

$$-\frac{1}{2}\varphi_{N-2} + \zeta_4\varphi_{N-1} - \zeta_5\varphi_N - \zeta_6\varphi_{N+1} + \frac{1}{2}\varphi_{N+2} = 0, \tag{20b}$$

$$\sigma_{N+1} = \sigma_{N-1} - \zeta_7\sigma_N. \tag{20c}$$

The coefficients ζ_i and μ_i can be found in Appendix A.

To close the system of equations (19) we turn to the boundary conditions at $\eta = 0$ and deal with the coupling between the disturbance equations. In the absence of the coupling at $\eta = 0$ the discretisation above simply leads to a penta-diagonal matrix equation for the φ_i; a simple iteration procedure can then be used to solve for the eigenvalues. In the presence of the boundary coupling such a scheme is not suitable and an alternate strategy is necessary. To proceed, let us introduce an unknown function H defined such that $\varphi''(0) = H$. We will normalise all dependent variables in (13)–(15) with respect to H; for instance $\varphi = H\tilde{\varphi}$ so that $\tilde{\varphi}''(0) = 1$. Due to the linearity of system (12) this normalization leaves the equations unchanged except for the fact that φ and σ are replaced by $\tilde{\varphi}$ and $\tilde{\sigma}$. Further, let us suppose that the value of $\tilde{\sigma}'$ is known at the boundary and denote it by D; its value must, of course, be found as part of the solution procedure. The boundary conditions (13)–(15) can then be written as

$$\tilde{\varphi}(0) = \frac{1.720\theta}{ScR_\delta}D, \quad \tilde{\varphi}''(0) = 1, \quad \tilde{\sigma}'(0) = D; \tag{21}$$

$$\tilde{\varphi}(\infty) = 0, \quad \tilde{\varphi}'(\infty) = 0, \quad \tilde{\sigma}(\infty) = 0.$$

For fixed values of Sc, R_δ, θ and A the "eigenvalues" will be deemed found if the remaining two boundary conditions $\tilde{\sigma}(0) = 0$ and $\tilde{\varphi}'(0) = 0$ are satisfied. This forms the basis of our iterative procedure for the determining the eigenvalues of the Orr–Sommerfeld system. For the sake of convenience, we shall omit the tilde from our notation in what follows.

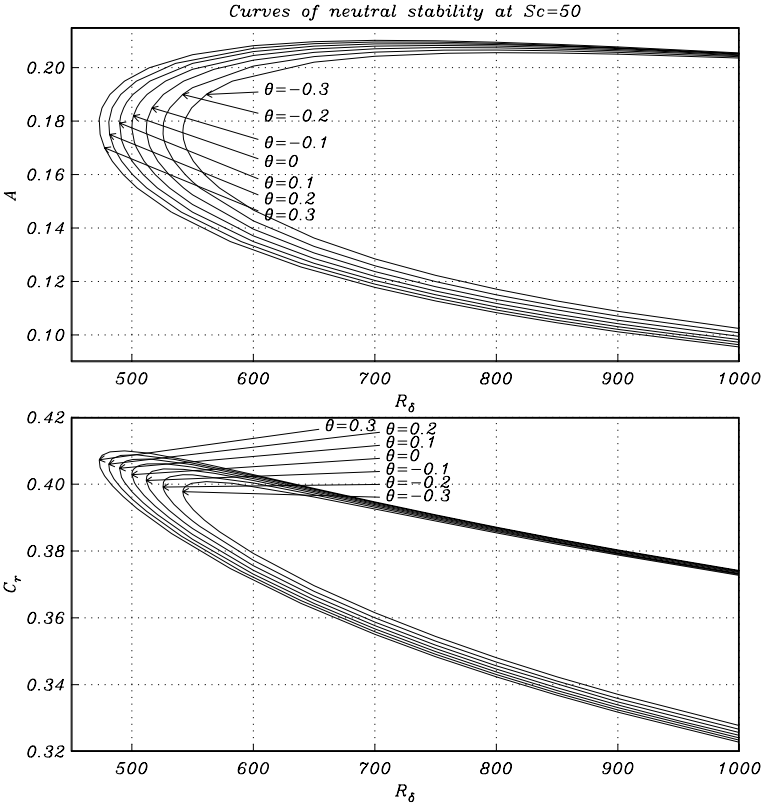

Fig. 6. Curves of neutral stability at $Sc = 50$ for different values of θ. The upper plot shows the neutral curves in the (R_δ, A)-plane whereas the lower plot gives the corresponding curves in the (R_δ, c_r)-plane.

Discretising the boundary conditions (13)–(15), and making use of (21), gives

$$\varphi_0 = \frac{1.72\theta}{ScR_\delta} D, \tag{22a}$$

$$\varphi_{-1} = \frac{3.44\theta}{ScR_\delta} D - \varphi_1 + h^2, \tag{22b}$$

$$\sigma_{-1} = \sigma_1 - 2hD, \tag{22c}$$

where we have introduced the false grid point η_{-1} in order to retain second order accuracy in η. To proceed we first set up initial guesses for the eigenvalue c and the unknown D at given values of R_δ, A, Sc and θ. The system of linear equations comprising (20)–(22) is solved for φ_j and σ_j $(j = 1, \ldots, N)$. We then iterate on c and D until $\varphi'(0) = 0$ and $\sigma(0) = 0$ are satisfied. The result is the eigenvalue $c = c_r + ic_i$ together with the unknown D and the corresponding eigenfunctions φ and σ.

5. Results and discussion

The system of equations governing the disturbance fields was solved using the algorithm described above to generate curves of neutral stability in (R_δ, A) and (R_δ, c_r) plane on which $c_i = 0$. These are presented in Figs. 4–7. Following the usual convention, the curves of neutral stability delineate the boundary in the parameter space between stable and unstable disturbances. The flow is unstable for values of the parameter that lay inside the neutral curve and stable outside. The calculations have been carried out at fixed Schmidt number ($Sc = 0.7$, 1, 50, 100) for different values of mass-transfer parameter θ. Note that the results for $\theta = 0$ correspond to the case of no mass transfer (that is, the Blasius boundary-layer flow over an impermeable flat plate). There is no coupling between the momentum and concentration fields and the classical results concerning the linearized stability of the Blasius flow are reproduced. Furthermore, we note that for the limiting case $\theta = 0$, the change in concentration within the boundary layer occurs simply through the passive mechanism of diffusion.

Returning to Fig. 4 we observe that fixing the Schmidt number Sc and decreasing the mass-transfer parameter θ (from positive through to negative values) serves to stabilise the flow by increasing the critical Reynolds number required for instability. This trend holds for all Schmidt numbers as evidenced by the

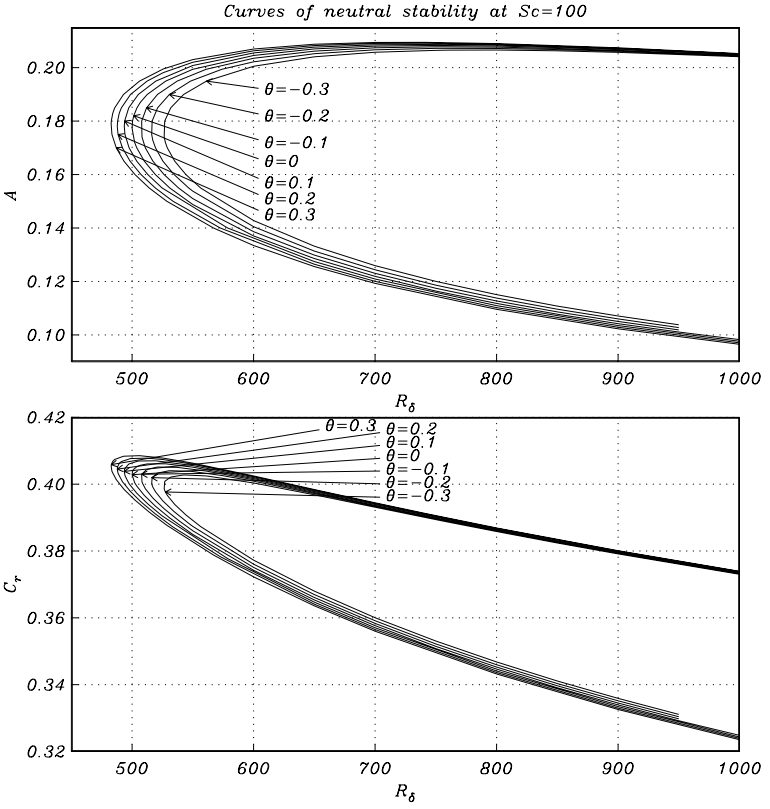

Fig. 7. Curves of neutral stability at $Sc = 100$ for different values of θ. The upper plot shows the neutral curves in the (R_δ, A)-plane whereas the lower plot gives the corresponding curves in the (R_δ, c_r)-plane.

curves presented in Figs. 5–7. Comparing the results in these figures for θ positive and negative demonstrates that the stabilizing effect of suction (i.e. $\theta < 0$) is more significant than the corresponding destabilising nature of blowing ($\theta > 0$). The destabilizing effect of the mass transfer directed into the boundary layer ($\theta > 0$) arises due to the addition of momentum through the coupling of the concentration and the flow velocity in Eq. (15).

From Fig. 4 we see that the effect of positive mass transfer (i.e. blowing from the substrate into the flow) is to decrease the critical Reynolds number. As a consequence the streamwise position at which the flow becomes unstable moves towards the leading edge of the plate. This in turn hints at the possibility of an early transition to turbulence induced by the mass transfer. This conclusion is in general agreement with the work [3–5,12] but corrects the errors which arise due to the approximations of decoupling between the disturbance fields. Comparing our results with those from Ref. [3] we find that, in the case $Sc = 0.7$, the critical Reynolds number, for a value of $\theta = -0.3$, is 2.1926×10^3 as compared to the value of 2.2322×10^3. For $\theta = 0.3$ the respective values are 2.2100×10^2 (current results) and 2.1841×10^2 (results of [3]). Thus the approximate results obtained by decoupling the boundary conditions under-predict the correct critical Reynolds number in cases when $\theta > 0$ and over-predict its value when $\theta < 0$. These differences are summarised in Fig. 8. Further, from Fig. 4 we observe that mass-transfer in the form of blowing serves to increase both the critical wavenumber and wave-speed. These general conclusions also hold for higher values of the Schmidt number as is demonstrated by the plots in Figs. 6 and 7. For ease of reference, the changes in the critical Reynolds number, wavenumber and wave-speed as a function of θ are summarised in Table 1.

The results presented in Table 1 demonstrate that, as was the case for the basic flow, the higher the Schmidt number Sc the less significant is the influence of the interfacial mass transfer on the stability of the flow. This is, perhaps, not surprising given the fact that the Schmidt number plays a role analogous to the Prandtl number in heat transfer. Thus for large Schmidt numbers the concentration boundary layer is much thinner than the momentum boundary layer and therefore the effect of mass transfer is relatively weak, except in the vicinity of the boundary. It is also important to note that, in the case of the disturbance equations, the magnitude (or extent) of the coupling between the momentum and concentration field, see (14), can be measured

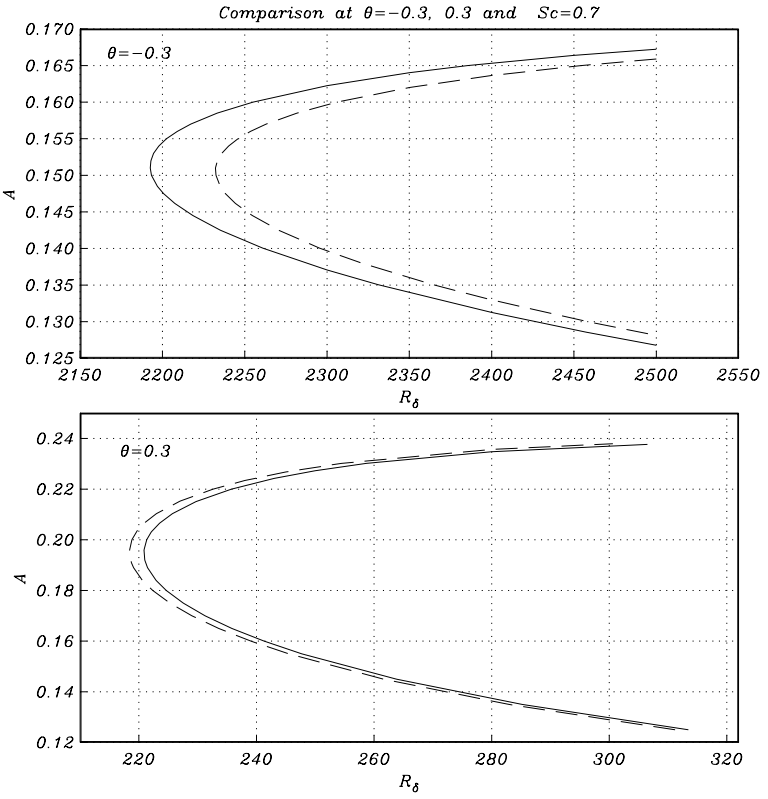

Fig. 8. Comparison between the present results and those of Ref. [3] (dashed curve).

Table 1
Values of critical Reynolds number R_δ, corresponding wave speed c_r and wavenumber A at $Sc = 0.7$, 1.0, 50, 100

θ	R_δ	A	c_r	R_δ	A	c_r
$Sc = 0.7$				$Sc = 1$		
−0.3	2192.6	0.151	0.3116	1604.9	0.155	0.3295
−0.2	1219.6	0.160	0.3462	1007.6	0.165	0.3585
−0.1	746.2	0.170	0.3772	685.8	0.170	0.3820
0.0	500.0	0.177	0.4028			
0.1	361.02	0.184	0.4242	385.0	0.183	0.4201
0.2	276.3	0.188	0.4414	309.5	0.190	0.4356
0.3	221.0	0.192	0.4563	257.0	0.190	0.4466
$Sc = 50$				$Sc = 100$		
−0.3	541.9	0.1762	0.3977	526.4	0.174	0.3985
−0.2	525.6	0.1752	0.3991	516.1	0.175	0.4001
−0.1	511.7	0.1763	0.4011	507.8	0.180	0.4029
0.1	489.9	0.1793	0.4047	493.5	0.178	0.4038
0.2	480.9	0.1797	0.4059	487.8	0.178	0.4045
0.3	473.1	0.1807	0.4073	482.7	0.179	0.4055

through the parameter $1/(ScR_\delta)$. Thus, when the combination ScR_δ is large the coupling is weak and the only significant influence of the mass transfer on the stability of the flow comes through its effect on the underlying boundary layer. In particular, in the case of large Schmidt number the results of Boyadjiev et al. [3,4,12] be-

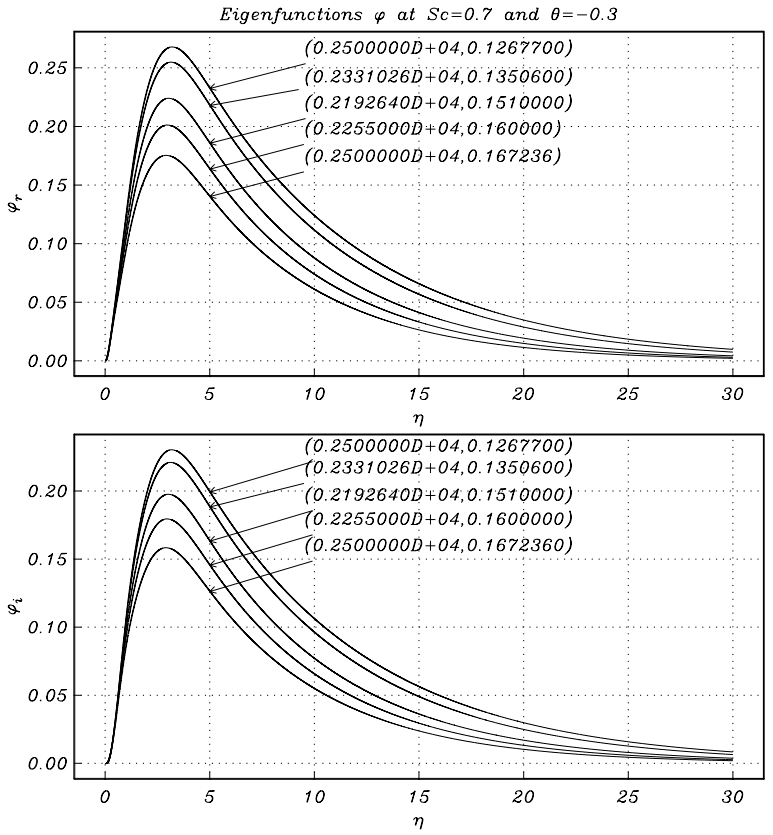

Fig. 9. The real φ_r and imaginary φ_i components of the eigenfunction φ at $Sc = 0.7$ and $\theta = -0.3$ at certain points on the neutral curve.

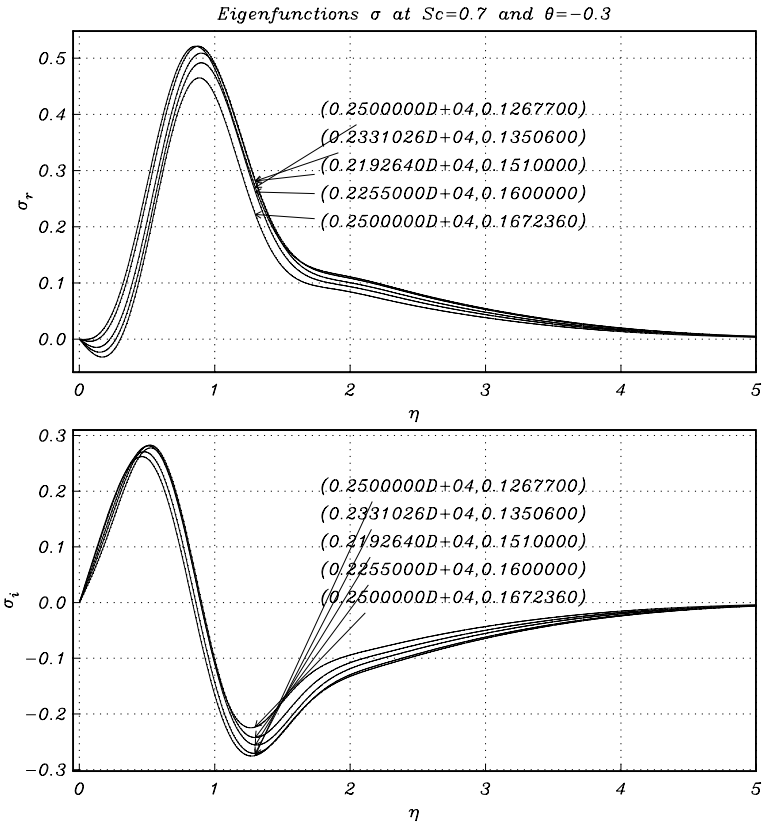

Fig. 10. The real σ_r and imaginary σ_i components of the eigenfunction σ at $Sc = 0.7$ and $\theta = -0.3$ at certain points on the neutral curve.

come a useful approximation for the critical flow parameters for the onset of instability.

Finally, the eigenfunctions $\varphi = \varphi_r + i\varphi_i$ and $\sigma = \sigma + i\sigma_i$ for the choice $Sc = 0.7$ and $\theta = -0.3$ for certain points on the neutral curve are presented in Figs. 9 and 10. In the range of the Reynolds numbers and mass-transfer rates presented, the coupling has a relatively minor effect on the initial value, $\varphi(0)$, of the disturbance velocity field. However, the eigenfunctions are exact (in the sense of a second-order accurate numerical scheme). Being able to obtain the correct form of the eigenfunctions (in this case, the perturbation streamfunction) is of utmost importance when considering the question of non-linear disturbances to the flow. Whether the flow is sub- or super-critically stable can only be answered by determining the associated coefficients in a Landau-type equation. These coefficients depend sensitively upon the critical Reynolds number, the critical wave-number and the associated eigenfunctions arising out of the linear stability analysis as presented here (see Drazin and Reid [8]). Any, non-quantifiable, error in these quantities will lead to inaccurate predictions as to the state of the non-linearly saturated flow.

If we look at this problem from a practical standpoint, as distinct from the theoretical one of explaining how and why the flow becomes unstable, then the critical requirement of any such linearized stability analysis is to be able to accurately predict the streamwise location at which the flow becomes unstable. The current work allows us to do this within the context of boundary-layer flows influenced by significant levels of (diffusion induced) mass transfer.

6. Conclusions

We have considered the problem of instability of the boundary-layer flow over a permeable surface under conditions of intense interfacial mass transfer. The full equations governing a small amplitude disturbance to the basic boundary-layer flow were derived and solved numerically using a modified version of a classical technique for solving two-point boundary-value problems.

We have been able to correct the earlier results of [3] and consistently account for the effect of coupling

between the momentum and concentration fields. At a fixed Schmidt number the flow is found to be increasingly unstable as the level of mass transfer is increased. The concomitant changes in the critical values of the wavenumber and wave-speed have also been obtained.

The difference between our results and the earlier results on Boyadjiev et al. [3,4,6,12], which were obtained via an ad hoc decoupling of the disturbance momentum and concentration fields, is of the order of 1% in terms of the critical Reynolds number. Although such a difference seems small, from the physical standpoint of predicting the onset of transition to turbulence, any such inaccuracy will lead to an erroneous result.

Finally we note that the importance of using the correct boundary conditions (that is, the fully coupled ones) is tantamount if one is to correctly capture the true physics of the instability process. For example, in the current (correct model) a disturbance in the concentration field induces a disturbance in the momentum field through the wall boundary condition (that is, the mass transfer due to molecular transport is an active process). Ignoring this effect gives results that are both mathematically and physically incorrect.

Work is currently underway to extend these results to account for finite amplitude effects in the flow. We hope to be able to report on this work in the near future.

Acknowledgements

This work was undertaken while IAH was a recipient of a University of Adelaide Research Scholarship. IAH also acknowledges the support of the Australian Research Council.

Appendix A. The coefficients of the discretized equations

In this appendix we present the coefficients appearing in the discretization of the coupled Orr–Sommerfeld system (19)–(22).

The coefficients a_i and b_j, $(i = 1,\ldots,4,\ j = 1,\ldots,3)$:

$$a_1 = -\frac{1}{2}(\eta f' - f), \quad a_2 = -2A^2 - \frac{\mathrm{i}AR_\delta}{1.720}(f' - c),$$

$$a_3 = \frac{1}{2}[(\eta f''' + f'') + A^2(\eta f' - f)],$$

$$a_4 = \left\{A^4 + \frac{\mathrm{i}AR_\delta}{1.720}[A^2(f' - c) + f'']\right\},$$

$$b_1 = -\frac{1}{2}Sc(\eta f' - f) = Sca_1,$$

$$b_2 = -A^2 - \frac{\mathrm{i}AR_\delta Sc}{1.720}(f' - c), \quad b_3 = \frac{AR_\delta Sc}{1.720}g'.$$

The coefficients μ_j appearing in (19) are given by

$$\mu_1 = -\frac{1}{h^3}\left(\frac{1}{2}a_1 - \frac{1}{h}\right),$$

$$\mu_2 = -\frac{1}{2h}a_3 + \frac{1}{h^2}a_2 + \frac{1}{h^3}a_1 - \frac{4}{h^4},$$

$$\mu_3 = a_4 - \frac{2}{h^2}a_2 + \frac{6}{h^4},$$

$$\mu_4 = \frac{1}{2h}a_3 + \frac{1}{h^2}a_2 - \frac{1}{h^3}a_1 - \frac{4}{h^4},$$

$$\mu_5 = \frac{1}{h^3}\left(\frac{1}{2}a_1 + \frac{1}{h}\right), \quad \mu_6 = -\frac{1}{h^3}\left(\frac{1}{2}b_1 - \frac{1}{h}\right),$$

$$\mu_7 = \frac{1}{h^2}\left(b_2 - \frac{2}{h^2}\right), \quad \mu_8 = \frac{1}{h^3}\left(\frac{1}{2}b_1 + \frac{1}{h}\right), \quad \mu_9 = \frac{1}{h^2}b_3,$$

and the coefficients appearing in (20) are

$$\zeta_1 = \frac{1}{2}h^2A^2 + h\chi_1 + 1, \quad \zeta_2 = h\chi_1(h^2A^2 + 2),$$

$$\zeta_3 = \frac{1}{2}h^2A^2 - h\chi_1 + 1,$$

$$\zeta_4 = \frac{1}{2}h^2\chi_3 + h\chi_2 + 1, \quad \zeta_5 = h(h^2Ay\beta_0^2 + 2\chi_2),$$

$$\zeta_6 = \frac{1}{2}h^2\chi_3 - h\chi_2 + 1, \quad \zeta_7 = 2h\chi_4,$$

where we have defined

$$\chi_1 = \frac{1}{4}\sqrt{k^2 + 16\beta_0^2} - \frac{1}{4}k, \quad \chi_2 = A - \frac{1}{2}k,$$

$$\chi_3 = \beta_0^2 + \frac{1}{2}Ak, \quad \chi_4 = \frac{1}{4}\sqrt{Sc^2k^2 + 16\beta_1^2} - \frac{1}{4}Sck.$$

References

[1] M. Abramowitz, I.A. Stegun, Handbook of Mathematical Functions, Dover Publications Inc, 1972, p. 877.
[2] R.B. Bird, W.E. Stewart, E.N. Lightfoot, Transport Phenomena, John Wiley, 2001.
[3] C.B. Boyadjiev, I.A. Halatchev, B. Tchavdarov, The linear stability in systems with intensive inter-phase mass transfer—I. Gas(liquid)–solid, Int. J. Heat Mass Transfer 39 (12) (1996) 2571–2580.
[4] C.B. Boyadjiev, I.A. Halatchev, The linear stability in systems with intensive inter-phase mass transfer—II. Gas–liquid, Int. J. Heat Mass Transfer 39 (12) (1996) 2581–2585.
[5] C.B. Boyadjiev, I.A. Halatchev, The linear stability in systems with intensive inter-phase mass transfer—IV. Gas–liquid film flow, Int. J. Heat Mass Transfer 39 (12) (1996) 2593–2597.
[6] C.B. Boyadjiev, N. Vulchanov, Influence of the intensive inter-phase mass transfer on the rate of mass transfer—1. The system "solid–fluid(gas)", Int. J. Heat Mass Transfer 33 (12) (1990) 2039–2044.

[7] R.A. Brewster, B. Gebhart, Instability and disturbance amplification in a mixed-convection boundary layer, J. Fluid Mech. 229 (1991) 115–133.
[8] P.G. Drazin, W.H. Reid, Hydrodynamic Stability, Dover Cambridge University Press, Cambridge, 1981.
[9] H.R. Lee, T.S. Chen, B.F. Armaly, Non-parallel thermal instability of forced convection flow over a heated, non-isothermal horizontal flat plate, Int. J. Heat Mass Transfer 33 (1990) 2019–2028.
[10] M.J. Krane, W.P. Buchanan, The hydrodynamic stability of a one-dimensional transient buoyancy-induced flow, Int. J. Heat Mass Transfer 36 (4) (1993) 977–988.
[11] B. Gebhart, H. Bau, R. Greif, Y. Jaluria, R.L. Mahajan, R. Viskanta, Thermal and Mass Diffusion Driven Flows, Research Trends in Fluid Dynamics, American Institute of Physics, 1996, pp. 77–91.
[12] I.A. Halatchev, C.B. Boyadjiev, The linear stability in systems with intensive inter-phase mass transfer—III. Liquid–Liquid, Int. J. Heat Mass Transfer 39 (12) (1996) 2587–2592.
[13] J.P. Hartnett, E.R.G. Eckert, Mass-transfer cooling in a laminar boundary layer with constant fluid properties, Trans. ASME 79 (1957) 247–254.
[14] H.B. Keller, Numerical Solution of Two Point Boundary Value Problems, SIAM Regional Conference Series in Applied Mathematics, Society for Industrial and Applied Mathematics, Philadelphia, 1976, pp. 56–58.
[15] E.W. Mureithi, J.P. Denier, J.A.K. Stott, The effect of buoyancy on upper branch Tollmien–Schlichting waves, IMA J. Appl. Math. 58 (1997) 19–50.
[16] H. Schlichting, Boundary-Layer Theory, McGraw-Hill Inc, 1979, p. 467.